Coherent Control of Causal Order of Entanglement Distillation

Zai Zuo,* Michael Hanks, and M. S. Kim QOLS, Blackett Laboratory, Imperial College London, SW7 2AZ, United Kingdom (Dated: March 14, 2023)

We present an application of indefinite causal order in quantum communication: a compound entanglement distillation protocol which features two steps of a basic distillation protocol applied in a coherent superposition of two causal orders. This is achieved by using one faulty entangled pair to control-swap two others before a fourth pair is combined with the two swapped ones consecutively. As a result, the protocol distills the four faulty entangled states into one of a higher fidelity. Our protocol has a higher fidelity of distillation and probability of success for some input faulty pairs than conventional concatenations of the basic protocol that follow a definite distillation order. Our proposal shows advantage of indefinite causal order in an application setting consistent with the requirements of quantum communication.

I. INTRODUCTION

Causality is a fundamental concept in nature and deeply embedded in the traditional model of computation. A computing algorithm, classical or quantum, usually envisions a target system undergoing a series of gates in a fixed causal order. Recent studies [1] revealed that under the assumption that quantum mechanics is valid locally, events can happen in an indefinite causal order (ICO). This concept was then extended to a quantum computation model with an indefinite causal structure (ICS), which features quantum operations occurring in an indefinite causal order [2, 3].

Significant effort was then made to look for specific computation and communication tasks where indefinite causal structures provide advantage. On the computation side, the Fourier [4, 5] and Hadamard promise problems [6, 7] were shown to enjoy a reduction in query complexity when quantum gates were queried through an indefinite causal order. On the communication side, some probabilistic communication tasks were found to result in a boost in success probability [8] and reduction in communication complexity [9] when passage order of information through communication parties was put into a superposition. It was also discovered that putting two noisy channels through a superposition of passage orders reduces noise of communication and for some specific channels results in complete noise removal [10–14]. The above examples of indefinite causal order all arise under the setup that two events, each of which is described by a completely positive (CP) map, are passed through by the target system in an order coherently controlled by another qubit. Mathematically, the advantage of putting CP maps in an indefinite causal order arises from the nonzero commutation and/or anti-commutation of Kraus operators that make up each quantum map [11, 15, 16].

An intriguing question that naturally arises is whether indefinite causal structures are useful in any current existing applications, which is the concern of this paper. Information-theoretic tasks that were studied in previous works [4-9] are not immediately generalizable to common computational tasks and algorithms and significant research effort is still required to bridge the gap. Studies that suggest noise reduction from superposition of passage orders of noisy channels [10–14] have assumed the message making a noiseless return to the head of the other channels after passing through one, which is inconsistent with realistic situations of quantum communication. To look for applications of indefinite causal structures, we take a different route which starts from the top by looking for existing computational tasks that may benefit from it under some modifications of their circuits. We suspect this is likely to be the case if the task features some subroutine which a quantum state undergoes repeatedly, each time interacting with some ancillary states. We have noticed a recently studied example [17–19] which was concerned with two noisy quantum teleportation steps carried out with pure but imperfect entangled pairs upon generation. They suggest that applying the two teleportation steps in an indefinite causal order by coherently swapping the two entangled pairs reduces noise on the teleported state. However, as we show in the Appendix of this paper, their proposal does not achieve noise reduction. In the more general case where noise occurs during the process of distribution of entanglement, swapping of the entangled pairs must be done remotely. This requires extra entanglement which brings difficulties to the proposal. It therefore remains unknown how useful indefinite causal structures are in existing computation and communication tasks.

In this paper, we show that distillation of entanglement, which is a basic and necessary task in quantum communication, benefits from indefinite causal structure. More specifically, it allows the production of higher-fidelity entangled pairs than merely carrying out distillation steps in a definite causal order. We consider the well-known entanglement distillation protocol proposed by Deutsch et.al. [20] (to be referred to as the DEJMPS protocol) which turns two faulty entangled pairs into one of a higher fidelity. When three faulty pairs, χ_i where $i \in 1, 2, 3$, are subject to such a protocol, χ_1 can be combined with χ_2 before the distillation product is combined

^{*} zai.zuo17@imperial.ac.uk

with pair χ_3 , or that χ_1 can be merged with χ_3 then χ_2 . This defines an "order" of entanglement distillation. We describe a protocol where the two orders are put into a coherent superposition and show that like other previously studied cases of indefinite causal order, the advantage in fidelity also comes from non-trivial commutation of Kraus operators of the CP map that describes the entanglement distillation. We then show the practical advantage of our protocol by presenting that for some input faulty entangled states, characterised by amount of mixture of the four Bell states, our protocol results in a higher fidelity and/or success probability than merely putting two distillation steps in a definite causal order. Given the known connection of entanglement distillation protocols and quantum error correction codes [21], we hope this work will stimulate effort into looking for the advantage of indefinite causal structures in quantum error correction.

This paper is organised as follows. In section II we review the basic principles of recent applications of indefinite causal order in the form of a quantum switch. In section III, we first review the DEJMPS entanglement distillation protocol, then present a naive modified protocol which performs two DEJMPS distillation steps in an superposed causal order. As the circuit of the proposed protocol is quite complicated, we then describe in section IV a simplified protocol which we show still simulates two DEJMPS distillation steps in superposed causal orders if we express the DEJMPS step using a different CP map. In section V we argue for our protocol by presenting the parameter regions of the input faulty states where our scheme shows an advantage over concatenations of DE-JMPS steps that follow a definite causal order. Some conclusions are then provided in section VI.

II. QUANTUM SWITCH AND COMMUTATIONS OF KRAUS OPERATORS OF QUANTUM OPERATIONS

A common framework to realise indefinite causal order between two quantum operations on a target state is to use an additional qubit to control the orders of occurrences of operations, such that the different orders are correlated with different basis states of the control qubit. Such a setup is named a "quantum switch" in the literature. Here, we give a short review of the basic principles of proposed applications of the quantum switch. Quantum operations are mathematically described as completely positive (CP) trace-non-increasing maps. When two quantum operations $\mathcal{M} = \sum_i M_i \rho M_i^{\dagger}$ and $\mathcal{N} = \sum_j N_j \rho N_j^{\dagger}$ (where M_i and N_j are Kraus operators. A special case is when $\mathcal{M} = M \rho M$ and $\mathcal{N} = N \rho N$ are unitary operators) are put into a quantum switch controlled by a qubit ρ_c , the overall map on the control

and target states reads

$$\mathcal{D}(\rho_c, \rho) = \sum_{ij} W_{ij}(\rho_c \otimes \rho) W_{ij}^{\dagger} \tag{1}$$

where the overall set of Kraus operators reads $W_{ij} = |0\rangle\langle 0| \otimes M_j N_i + |1\rangle\langle 1| \otimes N_i M_j$.

Previous works that studied using a quantum switch [22] to boost the communication capacity of noisy channels [10–13, 23] often initialise the control state as $\rho_c = |+\rangle\langle+|$, an even superposition of passage orders through the two quantum maps giving a resulting state

$$\mathcal{D}(\rho_c, \rho) = \frac{|+\rangle\langle+|}{2} \otimes \sum_{ij} (2M_j N_i \rho N_i M_j + 2N_i M_j \rho M_j N_i + [M_j, N_i] \rho [M_j, N_i]) + \frac{|-\rangle\langle-|}{2} \otimes \sum_{ij} (-[M_j, N_i] \rho [M_j, N_i]).$$

$$(2)$$

 ρ_c is then measured in the Fourier $(\{|+\rangle, |-\rangle\})$ basis and the state correlated with the $|+\rangle$ measurement outcome is post-selected. The benefit of having a quantum switch is due to non-trivial commutations of the set of Kraus operators $\{M_j\}$ and $\{N_i\}$ $([M_j,N_i]\neq 0$ for some i,j). To see why this is the case, suppose the opposite is true, i.e. $[M_j,N_i]=0$ for all i,j, then (2) is equal to $|+\rangle\langle+|\otimes\sum_{ij}M_jN_i\rho N_i^{\dagger}M_j^{\dagger},$ which is simply the case of ρ passing through two channels in a definite causal order.

III. DEJMPS PROTOCOL AND MODIFICATION

Entanglement distillation is a basic task in quantum communication that seeks to improve the quality of faulty entangled pairs distributed via noisy processes. A two-way entanglement distillation protocol [21] involves local unitary operations, local measurements and post-selections. Mathematically it can be described as a CP trace-decreasing map on the input state. In this section, we introduce the relevant notations. The DEJMPS protocol is also described to make the paper self-contained. In section III B and IV, we present two entanglement distillation protocols modified from the DEJMPS protocol [20]. The modified protocols feature two steps of the DEJMPS protocol applied in a superposition of two causal orders.

We adopt a common assumption that the faulty pairs χ_i are mixtures of Bell states [24]:

$$\chi_{i} = A_{i} |\Phi^{+}\rangle \langle \Phi^{+}| + B_{i} |\Psi^{-}\rangle \langle \Psi^{-}| + C_{i} |\Psi^{+}\rangle \langle \Psi^{+}| + D_{i} |\Phi^{-}\rangle \langle \Phi^{-}|$$
(3)

where

$$|\Phi^{\pm}\rangle = \frac{1}{\sqrt{2}}(|00\rangle \pm |11\rangle) \tag{4}$$

$$|\Psi^{\pm}\rangle = \frac{1}{\sqrt{2}}(|01\rangle \pm |10\rangle).$$
 (5)

Alternatively, it is compactly expressed as a column vector: $\chi_i = (A_i, B_i, C_i, D_i)^{\mathrm{T}}$ where T denotes the vector transpose. We define the fidelity of χ_i as

$$F = \max_{|B\rangle \in \{|\Phi^{\pm}\rangle, |\Psi^{\pm}\rangle\}} \langle B|\chi_i|B\rangle \tag{6}$$

When χ_i is given in equation (3), $F(\chi_i) = \max\{A_i, B_i, C_i, D_i\}.$

A. DEJMPS Distillation Protocol

The DEJMPS protocol [20] is one of the first proposed entanglement distillation schemes. Two faulty entangled pairs with density matrices χ_0 and χ_1 are shared. We denote the Hilbert space of χ_0 as $\mathcal{H}_0 = \mathcal{H}_{0A} \otimes \mathcal{H}_{0B}$ where Hilbert space \mathcal{H}_{0A} contains the state of the particle of χ_0 held by Alice and \mathcal{H}_{0B} contains that held by Bob. Likewise, we define $\mathcal{H}_1 = \mathcal{H}_{1A} \otimes \mathcal{H}_{1B}$ for the two particles of χ_1 . The DEJMPS protocol probabilistically turns the two faulty pairs into one entangled pair of a higher fidelity. The protocol has a circuit shown in figure 1 and is described as follows:

- Alice performs a rotation $\hat{R} = \exp(-i\frac{\pi}{2}\hat{X})$ on the particles on her side. Bob performs the rotation $\hat{R}^{\dagger} = \exp(+i\frac{\pi}{2}\hat{X})$ on the particles on his side.
- Alice and Bob each performs a CNOT between the two particles on their sides respectively. The two CNOTs are controlled by (and also targetting) qubits in the same entangled pair,
- Alice and Bob measure the target qubits of their CNOTs in the computational basis. Alice then sends Bob her measurement result. If their results agree, the entangled state serving as control qubits in the previous CNOTs is kept. If their results differ, the control pair is discarded and they start over again. In either case, the target pair is also discarded.

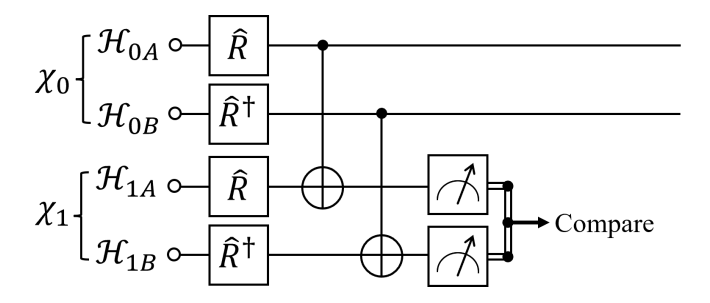


FIG. 1. The circuit for the DEJMPS entanglement distillation protocol. χ_1, χ_2 denote density matrices of the two shared entangled pairs. χ_i has its two particles sitting in Hilbert spaces \mathcal{H}_{iA} held by Alice and \mathcal{H}_{iB} held by Bob.

The CP trace-decreasing map which describes the above protocol can be expressed as

$$\mathcal{D}(\chi_0 \otimes \chi_1) = \sum_i \hat{O}^i(\chi_0 \otimes \chi_1) \hat{O}^{i\dagger} \tag{7}$$

where Kraus operators

$$\hat{O}^{i} = \langle i |_{1A,1B} \text{CNOT}_{0A}^{1A} \text{CNOT}_{0B}^{1B} \hat{R}_{0A,1A} \hat{R}_{0B,1B}^{\dagger}$$
 (8)

with $i \in \{00,11\}$. CNOT $_{0A}^{1A}$ is a CNOT gate with a control qubit in \mathcal{H}_{0A} and target qubit in \mathcal{H}_{1A} and $\hat{R}_{0A,1A} = \hat{R}_{0A} \otimes \hat{R}_{1A}$ where subscripts denote the Hilbert space of the operators. Equation (7) maps the combined input state in $\mathcal{H}_{0A} \otimes \mathcal{H}_{0B} \otimes \mathcal{H}_{1A} \otimes \mathcal{H}_{1B}$ onto the (unnormalized) output state in $\mathcal{H}_{0A} \otimes \mathcal{H}_{0B}$. The summation is a mixture over the two possible measurement outcomes 00 and 11 that show even parity.

Under the assumption of χ_0 and χ_1 both being Belldiagonal states, equation (7) can also be expressed as

$$\mathcal{D}'(\chi_0 \otimes \chi_1) = \hat{O}(\chi_0 \otimes \chi_1) \hat{O}^{\dagger} \tag{9}$$

where $\hat{O} = \sqrt{2}\hat{O}^{00}$. This simplification is justified by the fact that the measurement projecting the state in $\mathcal{H}_{1A} \otimes \mathcal{H}_{1B}$ onto $|11\rangle$ introduces an extra "-1" global phase onto the state in the leftover Hilbert space, and that the extra phases produced on both the "bra" and "ket" side cancel out. This makes projecting onto $|11\rangle$ equivalent as projecting onto $|00\rangle$.

In practice, the entangled pairs are used in various applications such as quantum clock synchronization [25], device-independent quantum key distribution [26, 27], quantum metrology [28] and distributed quantum computing [29]. These usage scenarios often request highfidelity entangled pairs, which can be obtained via repeated applications of single DEJMPS steps using x > 2faulty pairs. Alternatively, it may be viewed as a single faulty pair undergoing multiple steps of distillations, where each distinct step can be defined with respect to the entangled pair that the original one is combined with. We may then define the causal order of distillation to be the order with which the original pair is combined with others. As an example, for 3 faulty entangled states χ_i (where $i \in \{1, 2, 3\}$), we may distill χ_3 and χ_2 into a product of higher fidelity which is then distilled with χ_1 . The second distillation step is clearly in the causal future of the first step, as it requires the product of the first step as its input. Likewise, the first step is in the causal past of the second step.

An n-to-one distillation scheme when n>3 has more possible arrangements of single DEJMPS steps compared with the case when n=3. As an example, below are all the arrangements when n=4:

- No distillation is done. The pair of maximum fidelity out of the four is selected as the output.
- Do one distillation step using two of the four pairs. The two unselected pairs are discarded.

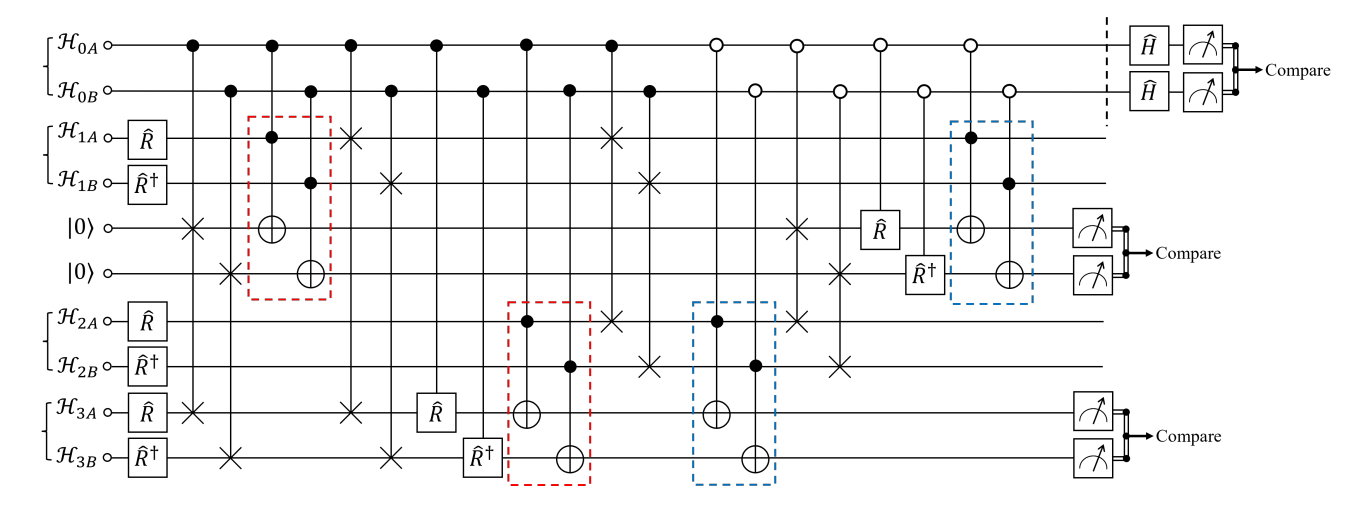


FIG. 2. A modified entanglement distillation scheme which turns four faulty Bell-diagonal states χ_i (each residing in Hilbert space $\mathcal{H}_{iA} \otimes \mathcal{H}_{iB}$) into one. The circuit features two DEJMPS distillation steps applied in a superposition of causal orders which is coherently controlled by the faulty pair χ_0 . The red (blue) dashed rectangles encircle the CNOT gates of the two DEJMPS steps applied in the $\chi_3 \to \chi_1 \to \chi_2$ ($\chi_3 \to \chi_2 \to \chi_1$) causal order. After the vertical dashed line in the figure, we post-select the distilled state upon receiving an even parity measurement outcome from the state in $\mathcal{H}_{0A} \otimes \mathcal{H}_{0B}$. This interferes the products distilled from the two causal orders with the hope of boosting the fidelity of the final product of distillation

- Select three out of four pairs and discard the fourth pair. Within the three chosen ones, select two to do one step of distillation, the product of which is teamed up with the third unchosen pair for another step.
- Group all four pairs into teams of two, where one step of distillation is carried out separately for each team before the two products are teamed up for another step. This is called a "recurrence-like structure" [30].
- Select two pairs to do one step of distillation, the product of which is purified by combining it with either of the two unchosen pairs before the product is combined with the last unchosen pair for a third step. This is called a "pumping-like structure" [30, 31].

For four faulty pairs χ_i (where $i \in \{0, 1, 2, 3\}$), we denote the set which contains all the above distillation arrangements as \mathcal{G} . All protocols $\mathcal{P} \in \mathcal{G}$ are examples of distillation steps carried out in a definite causal order, where the causal order between different steps are well defined. In the next subsection, we introduce our modification to break this causality.

B. A Circuit that Coherently Controls the Order of Two DEJMPS Steps

We consider the following process: the four Bell-diagonal faulty pairs χ_i s are shared between Alice and Bob as illustrated in figure 3. Under some control system being in a logical state $|\mathbf{0}\rangle$, χ_3 undergoes a DEJMPS

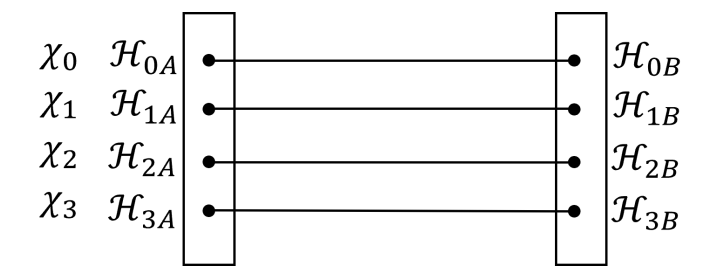


FIG. 3. Four faulty Bell-diagonal pairs are shared between two repeater stations. $\mathcal{H}_{x,Y}$ where $x \in \{0,1,2,3\}$ and $Y \in \{A,B\}$ denotes the Hilbert space of each stored qubit.

step with χ_2 first, whose distillation output then undergoes another DEJMPS step with χ_1 . When the control system is in $|\mathbf{1}\rangle$ orthonormal to $|\mathbf{0}\rangle$, χ_3 is routed in the quantum registers to first combine with χ_1 , whose distillation output is then combined with χ_2 . We let the logical states $|\mathbf{0}\rangle$ ($|\mathbf{1}\rangle$) be encoded in the entangled pair χ_0 as $|00\rangle$ ($|11\rangle$) and refer to χ_0 as the "control pair" of the protocol. The above process then can be realized by part of the circuit shown in figure 3 before the vertical dashed line. In figure 3, each entangled pair χ_i is inside Hilbert space $\mathcal{H}_{iA}\otimes\mathcal{H}_{iB}$. We denote $\rho_{\rm in}=\chi_1\otimes\chi_2\otimes\chi_3$. One can show before the vertical dashed line, the overall state in Hilbert space $\mathcal{H}_{0A}\otimes\mathcal{H}_{0B}\otimes\mathcal{H}_{1A}\otimes\mathcal{H}_{1B}$, which consists of the control pair and the bipartite state distilled from the two DEJMPS steps, can be expressed as

$$\rho_s = \sum_{i,j=00}^{11} \hat{E}_{ij}(\chi_0 \otimes \rho_{\rm in}) \hat{E}_{ij}^{\dagger} + \sum_{i,j=00}^{11} \hat{K}_{ij}(\chi_0 \otimes \rho_{\rm in}) \hat{K}_{ij}^{\dagger}$$
(10)

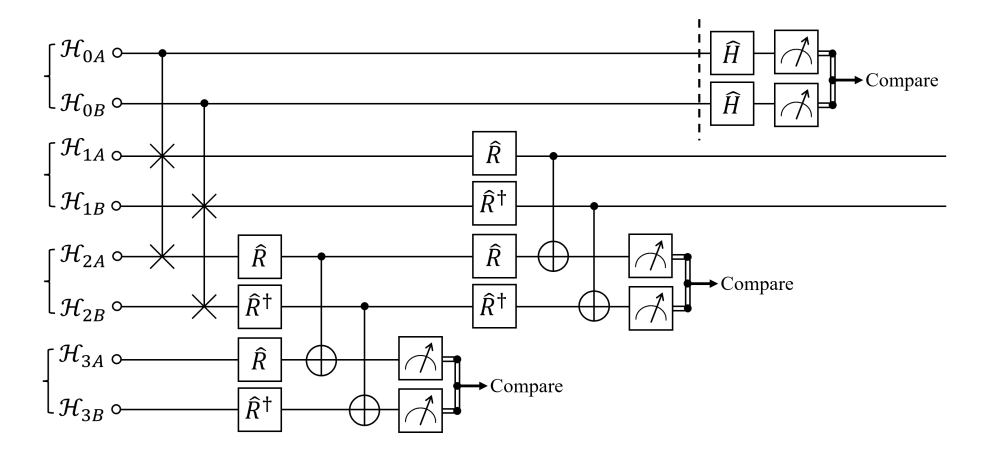


FIG. 4. A simpler circuit which seeks to simulate two DEJMPS steps in a coherent superposition of two causal order. This is achieved by coherent swapping of χ_1 and χ_2 at the beginning of the circuit, in contrast to figure 2 where χ_1 and χ_2 are kept still and χ_3 is routed around. Notations: $\hat{R} = \exp(-i\frac{\pi}{2}\hat{X})$ where \hat{X} is the Pauli-X operator. \hat{R}^{\dagger} is the Hermitian conjugate of \hat{R} . \hat{H} is the Hadamard gate.

where

$$\hat{E}_{ij} = |00\rangle\langle00| \otimes \hat{\mathcal{E}}_{i}^{(2)}\hat{\mathcal{E}}_{i}^{(1)} + |11\rangle\langle11| \otimes \hat{\mathcal{E}}_{i}^{(1)}\hat{\mathcal{E}}_{i}^{(2)}$$
 (11)

$$\hat{K}_{ij} = |01\rangle\langle 01| \otimes \hat{\mathcal{K}}_i^{(1)} + |10\rangle\langle 10| \otimes \hat{\mathcal{K}}_j^{(2)}. \tag{12}$$

with

$$\begin{split} \hat{\mathcal{E}}_i^{(1)} &= \text{SWAP}_{3A}^{2A} \text{SWAP}_{3B}^{2B} \\ & \qquad \langle i|_{3A,3B} \text{CNOT}_{2A}^{3A} \text{CNOT}_{2B}^{3B} \hat{R}_{2A,3A} \hat{R}_{2B,3B}^{\dagger} \end{split}$$

$$\begin{split} \hat{\mathcal{E}}_{j}^{(2)} &= \text{SWAP}_{3A}^{1A} \text{SWAP}_{3B}^{1B} \\ & \langle j|_{3A,3B} \text{CNOT}_{1A}^{3A} \text{CNOT}_{1B}^{3B} \hat{R}_{1A,3A} \hat{R}_{1B,3B}^{\dagger} \\ & (14) \end{split}$$

where SWAP $_{3A}^{2A}$ is a SWAP gate between the states in Hilbert spaces \mathcal{H}_{3A} and \mathcal{H}_{2A} . $\hat{\mathcal{K}}_i^{(1)}$ and $\hat{\mathcal{K}}_j^{(2)}$ are the operations on $\rho_{\rm in}$ in the case that the the control pair χ_0 is in the state $|01\rangle$ or $|10\rangle$. We do not give the explicit expression of $\hat{\mathcal{K}}_i^{(1)}$ and $\hat{\mathcal{K}}_j^{(2)}$ as they do not contribute to the discussion. $\hat{\mathcal{E}}_i^{(m)}$ is essentially the Kraus operator of a DEJMPS step as given in equation (7) but with extra SWAPs that do not affect outcome of distillation. $\hat{\mathcal{E}}_{ij}$ has the form of different basis states of the control pair correlated with opposite orders of $\hat{\mathcal{E}}_i^{(1)}$ and $\hat{\mathcal{E}}_j^{(2)}$, the Kraus operators of the two DEJMPS steps. This clearly shows that the two distillation steps are put into an indefinite causal order. The second term in equation (10) occurs when the control pair χ_0 has Bell components $|\Psi^+\rangle\langle\Psi^+|$ and/or $|\Psi^-\rangle\langle\Psi^-|$. This gives rise to another completely positive map which cannot be easily interpreted as χ_3 going through two DEJMPS steps in any order.

After the two DEJMPS steps, a Hadamard gate is applied onto both particles of the control pair, which is followed by a parity measurement on the control pair (shown in figure 2 after the vertical dashed line). We then

post-select the bipartite state in the unmeasured Hilbert space $\mathcal{H}_{1A} \otimes \mathcal{H}_{1B}$ over an even parity outcome. This allows the distillation product from the two causal orders to interfere and the state in the unmeasured Hilbert space is the final product of the protocol.

One sees from figure 2 that the circuit is quite complicated. It also requires the control pair to coherently control every gate within the DEJMPS protocol. This gives rise to a large number of double-controlled gates between three qubits, which are difficult to implement. These factors make the circuit difficult to demonstrate as an entanglement distillation protocol. In section IV, we introduce a much simpler circuit that also simulates two DEJMPS steps in an indefinite causal order. In this new circuit, the causal orders of DEJMPS steps are not emulated by routing χ_3 , but merely control-SWAPPING χ_1 and χ_2 . We show that the output state under this simplified protocol can be expressed as $\rho_{\rm in}$ undergoing two maps with set of Kraus operators defined in equation (9). The new circuit uses a smaller number of gates, and noticeably many fewer controlled gates among three particles. These features shall make the new circuit easier to demonstrate in practice.

IV. A SIMPLIFIED COHERENT CONTROL OF ORDER OF TWO DEJMPS STEPS

The simplified scheme of coherently controlling the order of two DEJMPS distillation steps has a circuit shown in figure 4 and is described as follows:

1. We apply a controlled-SWAP gate from the particle in Hilbert space \mathcal{H}_{0A} to the two particles in Hilbert spaces \mathcal{H}_{1A} and \mathcal{H}_{2A} . The particle in Hilbert space \mathcal{H}_{0B} performs a controlled-SWAP gate on the two particles in Hilbert spaces \mathcal{H}_{1B} and \mathcal{H}_{2B} . The controlled-SWAP gate is such that the two target

states are swapped if the control qubit is in $|1\rangle$.

- 2. We apply one step of DEJMPS protocol as described earlier in section III A on Hilbert spaces $\mathcal{H}_{3A} \otimes \mathcal{H}_{3B}$ and $\mathcal{H}_{2A} \otimes \mathcal{H}_{2B}$. If the measurement outcomes show even parity, \mathcal{H}_{2A} and \mathcal{H}_{2B} are kept and we proceed to step 3. Otherwise we discard all pairs and start the scheme over with newly supplied faulty pairs.
- 3. We apply another step of Deutsch's protocol on Hilbert spaces $\mathcal{H}_{2A} \otimes \mathcal{H}_{2B}$ and $\mathcal{H}_{1A} \otimes \mathcal{H}_{1B}$. If the parity measurement outcome is even, \mathcal{H}_{1A} and \mathcal{H}_{1B} are kept and we continue to step 4. Otherwise we discard all pairs and start again from the beginning.
- 4. We measure \mathcal{H}_{0A} and \mathcal{H}_{0B} separately in the Fourier $\{|+\rangle, |-\rangle\}$ basis and compare the results. If they show even parity, the scheme is successful. Otherwise we discard all pairs and start again from the beginning.

Despite we have described operations during the protocol as occurring among certain Hilbert spaces, the above protocol also works for other combinations of the Hilbert spaces. For example, the control-SWAP in step 1 can instead be controlled by particles in Hilbert spaces $\mathcal{H}_{1A} \otimes \mathcal{H}_{1B}$ which targets $\mathcal{H}_{2A} \otimes \mathcal{H}_{2B}$ and $\mathcal{H}_{3A} \otimes \mathcal{H}_{3B}$, then the two DEJMPS steps are carried out between states in $\mathcal{H}_{0A} \otimes \mathcal{H}_{0B} \& \mathcal{H}_{2A} \otimes \mathcal{H}_{2B}$ and $\mathcal{H}_{2A} \otimes \mathcal{H}_{2B} \& \mathcal{H}_{3A} \otimes \mathcal{H}_{3B}$. This variation defines a whole set of protocols (there are in fact 12 such protocols), which we denote as \mathcal{S} , each having a similar structure.

A. Difference Between Routing χ_3 And Swapping χ_1 & χ_2

One may be tempted to infer that the two circuits in figure 2 and 4 are equivalent: whether routing χ_3 around while keeping χ_2 and χ_1 still (in figure 2) or swapping χ_2 and χ_1 around while keeping χ_3 still (in figure 4) should not matter, as they both simulate χ_3 going through DE-JMPS distillations with χ_2 and χ_1 in two opposite orders. This is not actually the case, due to the parity measurements that are part of the distillation protocol. In figure 2's circuit, the two DEJMPS steps, each associated with χ_2 or χ_1 , can have different parity measurement results (00 or 11, under the even-parity requirement), and that the parity measurement results associated with χ_2 and χ_1 are the same for both causal orders (whether χ_2 is used after or before χ_1). In figure 4's circuit, however, the first DEJMPS steps (regardless of whether it is with χ_2 or χ_1) performed in both causal branches have the same parity measurement outcome, and so do the second DEJMPS steps in both causal branches. This means that if the CP trace-decreasing map of each DEJMPS step is expressed as equation (7), which is a sum over projections onto $|00\rangle$ and $|11\rangle$, the overall state before the vertical dashed line in figure 4's circuit cannot be

written as equation (10), where the effective Kraus operator \hat{E}_{ij} has components that are exact swapping of the Kraus operators of the two DEJMPS steps. We therefore cannot interpret the distillation output of figure 4's circuit as χ_3 going through two DEJMPS steps in an indefinite causal order, if the completely positive map of the DEJMPS protocol is given as equation (7).

B. Completely Positive Trace-decreasing Maps under Swapping of χ_1 and χ_2

In this section, we are able to show that figure 4's circuit can be interpreted as χ_3 undergoing two DEJMPS steps in an indefinite causal order, if the DEJMPS protocol is instead described by equation (9). We point out that for Bell-diagonal states as being considered in this paper, both (7) and (9) are equally valid quantum maps describing the DEJMPS protocol since mathematically they produce the exact distillation output as defined by the DEJMPS circuit [20]. In this section, we assume the control pair is χ_0 which control-SWAPs χ_1 and χ_2 . This makes $\rho_0 = \chi_0 \otimes \chi_1 \otimes \chi_2 \otimes \chi_3$ and $\rho_{\rm in} = \chi_1 \otimes \chi_2 \otimes \chi_3$.

Following the circuit in figure 4, one can show that at the dashed line before the final Hadamard gates and parity measurements, the state in $\mathcal{H}_{0A} \otimes \mathcal{H}_{0B} \otimes \mathcal{H}_{1A} \otimes \mathcal{H}_{1B}$ reads

$$\rho_{s} = \frac{A_{0} + D_{0}}{2} (|00\rangle\langle00| \otimes N_{1} + |11\rangle\langle11| \otimes N_{2}) + \frac{A_{0} - D_{0}}{2} (|00\rangle\langle11| \otimes M_{1} + |11\rangle\langle00| \otimes M_{2}) + \frac{B_{0} + C_{0}}{2} (|01\rangle\langle01| \otimes T_{1} + |10\rangle\langle10| \otimes T_{2}) + \frac{C_{0} - B_{0}}{2} (|01\rangle\langle10| \otimes L_{1} + |10\rangle\langle01| \otimes L_{2})$$

$$(15)$$

where

$$N_1 = \sum_{i,j \in 00,11} \hat{F}^j \hat{O}^i \rho_{\rm in} \hat{O}^{i\dagger} \hat{F}^{j\dagger}$$
 (16)

$$N_2 = \sum_{i,j \in 00,11} \hat{F}^j \hat{P}^i \rho_{\rm in} \hat{P}^{i\dagger} \hat{F}^{j\dagger}$$
 (17)

$$M_1 = \sum_{i,j \in 00,11} \hat{F}^j \hat{P}^i \rho_{\rm in} \hat{O}^{i\dagger} \hat{F}^{j\dagger}$$
 (18)

$$M_2 = \sum_{i,j \in 00,11} \hat{F}^j \hat{O}^i \rho_{\rm in} \hat{P}^{i\dagger} \hat{F}^{j\dagger}$$
 (19)

and

$$\hat{O}^{i} = \langle i |_{3A,3B} \text{CNOT}_{2A}^{3A} \text{CNOT}_{2B}^{3B} \hat{R}_{2A,3A} \hat{R}_{2B,3B}^{\dagger}$$
 (20)

$$\hat{P}^i = \hat{O}^i \text{SWAP}_{1A}^{2A} \text{SWAP}_{1B}^{2B} \tag{21}$$

$$\hat{F}^{j} = \langle j |_{2A,2B} \text{CNOT}_{1A}^{2A} \text{CNOT}_{1B}^{2B} \hat{R}_{1A,2A} \hat{R}_{1B,2B}^{\dagger}. \quad (22)$$

The explicit expressions of T_1, T_2, L_1 and L_2 are given in section IV C, which can be found by tracing the circuit in figure 4 in case the control pair is in state $|01\rangle$ or $|10\rangle$.

Theorem 1 N_1 and N_2 , the (unormalized) distillation product states from two DEJMPS steps in opposite causal orders can be expressed as

$$N_1 = \hat{Q}_2 \hat{Q}_1 \rho_{\rm in} \hat{Q}_1 \hat{Q}_2 \tag{23}$$

$$N_2 = \hat{Q}_1 \hat{Q}_2 \rho_{\rm in} \hat{Q}_2 \hat{Q}_1, \tag{24}$$

while M_1 and M_2 , the (unormalized) entangled states correlated with the off-diagonal terms between the two basis states of the control pair that control-swaps χ_1 and χ_2 , can be expressed as

$$M_1 = \hat{Q}_1 \hat{Q}_2 \rho_{\rm in} \hat{Q}_1 \hat{Q}_2 \tag{25}$$

$$M_2 = \hat{Q}_2 \hat{Q}_1 \rho_{\rm in} \hat{Q}_2 \hat{Q}_1, \tag{26}$$

where Kraus operators

$$\begin{split} \hat{Q}_1 = \sqrt{2}\langle 00|_{2A,2B} \text{SWAP}_{2A}^{3A} \text{SWAP}_{2B}^{3B} \text{CNOT}_{2A}^{3A} \text{CNOT}_{2B}^{3B} \\ \hat{R}_{2A,3A} \hat{R}_{2B,3B}^{\dagger} \end{split}$$

(27)

 $\hat{Q}_2 = \sqrt{2}\langle 00|_{1A,1B} \text{SWAP}_{1A}^{3A} \text{SWAP}_{1B}^{3B} \text{CNOT}_{1A}^{3A} \text{CNOT}_{1B}^{3B}$

$$\hat{R}_{1A,3A}\hat{R}_{1B,3B}^{\dagger} \tag{28}$$

are equivalent to the Kraus operator of a single DEJMPS step that only projects the parity-measured states onto $|00\rangle$, up to extra SWAP gates that relabel the Hilbert spaces of the subsystems.

Proof To show that N_1 , N_2 , M_1 and M_2 can be expressed as equations (23) to (26), two major steps are carried out. We first show that both outcomes of parity measurements (00 and 11) yield the same distillation output. This allows us to express mixture over projections onto "00" and "11" as only projecting onto "00". Secondly, we intersperse gates inside \hat{O}^i , \hat{P}^i and \hat{F}^i with additional SWAP gates to relabel some of the involved Hilbert spaces in order to arrive at \hat{Q}_1 and \hat{Q}_2 .

For convenience of description, we introduce a more compact notation that denotes χ_i as

$$\chi_i = \sum_{a,b} m_{a,b}^{(i)} |\beta_{a,b}\rangle \langle \beta_{a,b}|$$
 (29)

where $a \in \{0,1\}$ denotes the parity of the Bell component and $b \in \{0,1\}$ denotes the "+", "-" sign of the component such that $\{|\beta_{0,0}\rangle, |\beta_{1,1}\rangle, |\beta_{1,0}\rangle, |\beta_{0,1}\rangle\} = \{|\Phi^+\rangle, |\Psi^-\rangle, |\Psi^+\rangle, |\Phi^-\rangle\}$. $m_{a,b}^{(i)}$ s are the corresponding coefficients of the components which satisfy $\sum_{a,b} m_{a,b}^{(i)} = 1$ due to normalisation. The input faulty states $\rho_{\rm in}$ can be expressed as a mixture over components, each being a tensor product of three Bell states:

$$\rho_{\rm in} = \sum_{\mathbf{a}, \mathbf{b}} (\prod_i m_{a_i, b_i}^{(i)}) \Gamma_{\mathbf{a}, \mathbf{b}}$$
 (30)

where $\Gamma_{\mathbf{a},\mathbf{b}} = |\beta_{a_1,b_1}\rangle |\beta_{a_2,b_2}\rangle |\beta_{a_3,b_3}\rangle \times \text{h.c}$ and $\mathbf{a} = (a_1, a_2, a_3), \mathbf{b} = (b_1, b_2, b_3).$

It is not immediately clear that the two parity measurement outcomes (00 and 11) are correlated with equivalent output state and as a result, it is not clear that the sum over "00" and "11" in equations (16) to (19) can just be re-expressed as projecting only onto "00". To see this, we first examine the inner parts of N_1 , N_2 and M_1 : $\hat{O}^i\Gamma_{\mathbf{a},\mathbf{b}}\hat{O}^{i\dagger}$, $\hat{P}^i\Gamma_{\mathbf{a},\mathbf{b}}\hat{P}^{i\dagger}$ and $\hat{P}^i\Gamma_{\mathbf{a},\mathbf{b}}\hat{O}^{i\dagger}$ (M_2 is simply the Hermitian conjugate of M_1). These terms consist of initial rotations \hat{R} on two Bell states, CNOTs and projection onto $|00\rangle$ or $|11\rangle$. It is known from [20] that \hat{R} preserves the diagonal structure of $\Gamma_{\mathbf{a},\mathbf{b}}$: It merely permutes $|\Phi^-\rangle$ and $|\Psi^-\rangle$, leaving $|\Phi^+\rangle$ and $|\Psi^+\rangle$ unchanged. The trailing CNOT gates hence still act on a Bell-diagonal state. The CNOTs turn $|\beta_{a_2,b_2}\rangle|\beta_{a_3,b_3}\rangle$ into $|\beta_{a_2,b_2\oplus b_3}\rangle|\beta_{a_2\oplus a_3,b_3}\rangle$ and preserve the sign of the Bell state (b_3) in $\mathcal{H}_{3A} \otimes \mathcal{H}_{3B}$, where the subsequent first parity measurement is done. The sign of the Bell state b_3 is important. We note that projections of $|\Phi^+\rangle$ (the case where $b_3 = 0$) onto $|00\rangle$ and $|11\rangle$ both yield a trivial global phase. But for the "negative sign" $|\Phi^-\rangle$ (where $b_3 = 1$), projection onto $|00\rangle$ yields a trivial global phase, while projection onto |11\rangle yields a "-1" global phase. Here, since the terms $\hat{O}^i\Gamma_{\mathbf{a},\mathbf{b}}\hat{O}^{i\dagger}$, $\hat{P}^i\Gamma_{\mathbf{a},\mathbf{b}}\hat{P}^{i\dagger}$ and $\hat{P}^i \Gamma_{\mathbf{a}, \mathbf{b}} \hat{O}^{i\dagger}$ are correlated with the control pair being in $|00\rangle\langle00|$, $|11\rangle\langle11|$ and $|00\rangle\langle11|$, respectively (see equations (15) to (19)), the global phases generated during the parity measurement become relative phases among the above three terms, which can affect the final distilled state non-trivially. However, the fact that the CNOTs preserve the sign of the target Bell state means after the CNOTs, the Bell states on the "bra" and "ket" sides must have the same sign (b_3) regardless of the control Bell state of the CNOTs on the two sides. The global phases induced on the two sides cancel to give an overall "+1" phase, making the "00" and "11" outcomes have equivalent effect onto the leftover Hilbert space. Mathematically, the following relations are obtained: $\hat{O}^{00}\Gamma_{\mathbf{a},\mathbf{b}}\hat{O}^{00\dagger} = \hat{O}^{11}\Gamma_{\mathbf{a},\mathbf{b}}\hat{O}^{11\dagger}, \ \hat{P}^{00}\Gamma_{\mathbf{a},\mathbf{b}}\hat{P}^{00\dagger} = \hat{P}^{11}\Gamma_{\mathbf{a},\mathbf{b}}\hat{P}^{11\dagger} \text{ and } \hat{P}^{00}\Gamma_{\mathbf{a},\mathbf{b}}\hat{O}^{00\dagger} = \hat{P}^{11}\Gamma_{\mathbf{a},\mathbf{b}}\hat{O}^{11\dagger}.$

The leftover state in $(\mathcal{H}_{1A} \otimes \mathcal{H}_{1B}) \otimes (\mathcal{H}_{2A} \otimes \mathcal{H}_{2B})$, after tracing out $\mathcal{H}_{3A} \otimes \mathcal{H}_{3B}$, is also a tensor product of two Bell states, and is now subject to another round of local rotations, CNOTs and parity measurement. One can use the same argument as above to show that projecting onto $|00\rangle$ and $|11\rangle$ in the parity measurement yield the same state in the leftover Hilbert space $\mathcal{H}_{1A} \otimes \mathcal{H}_{1B}$. This means $\hat{F}^{00}\hat{\Omega}^i\Gamma_{\mathbf{a},\mathbf{b}}\hat{\Upsilon}^{i\dagger}\hat{F}^{00\dagger} = \hat{F}^{11}\hat{\Omega}^i\Gamma_{\mathbf{a},\mathbf{b}}\hat{\Upsilon}^{i\dagger}\hat{F}^{11\dagger}$ for $i \in \{00,11\}$, where $\hat{\Omega}$ and $\hat{\Upsilon}$ are either \hat{O} or \hat{P} . Since this is true for $\Gamma_{\mathbf{a},\mathbf{b}}$ of arbitrary \mathbf{a},\mathbf{b} , it is also true for ρ_{in} , which is a mixture of $\Gamma_{\mathbf{a},\mathbf{b}}$ of different \mathbf{a} and \mathbf{b} . We can now define $\hat{F} = \sqrt{2}\hat{F}^{00}$, $\hat{O} = \sqrt{2}\hat{O}^{00}$ and $\hat{P} = \sqrt{2}\hat{P}^{00}$ and express N_1 , N_2 , M_1 and M_2 as ρ_{in} going through single Kraus operators, rather than mixtures over Kraus operators that project onto different parity-measurement

outcomes 00 or 11:

$$N_1 = \hat{F}\hat{O}\rho_{\rm in}\hat{O}^{\dagger}\hat{F}^{\dagger} \tag{31}$$

$$N_2 = \hat{F}\hat{P}\rho_{\rm in}\hat{P}^{\dagger}\hat{F}^{\dagger} \tag{32}$$

$$M_1 = \hat{F}\hat{P}\rho_{\rm in}\hat{O}^{\dagger}\hat{F}^{\dagger} \tag{33}$$

$$M_2 = \hat{F}\hat{O}\rho_{\rm in}\hat{P}^{\dagger}\hat{F}^{\dagger}.\tag{34}$$

We now want to express N_1 as $\rho_{\rm in}$ passing through two CP trace-decreasing maps in one order, and N_2 as $\rho_{\rm in}$ undergoing the same two maps in the opposite order. We have defined a DEJMPS step, which has its distinct CP trace-decreasing map and Kraus operator, solely with respect to the entangled pair $(\chi_1 \text{ or } \chi_2)$ that χ_3 is combined with. In figure 4's circuit, however, the faulty state subject to the second distillation step (regardless of which entangled pair it is combined with) is in Hilbert space $\mathcal{H}_{2A} \otimes \mathcal{H}_{2B}$, which is different from the Hilbert space of χ_3 ($\mathcal{H}_{3A} \otimes \mathcal{H}_{3B}$) during the first distillation step. Since operations on distinct Hilbert spaces are described by different operators, this prevents the same Kraus operator that describes the 1st distillation step in one causal order from also describing the 2nd distillation step in the other causal order. To resolve this, we add extra SWAP operations to F, O and P such that the state produced from each DEJMPS step is always in Hilbert space $\mathcal{H}_{3A} \otimes \mathcal{H}_{3B}$, regardless of whether the DEJMPS step is done as the first or second in the queue. Consider the term N_1 . We add two SWAP gates $SWAP_{2A}^{3A}SWAP_{2B}^{3B}$ between the CNOTs and parity measurement of operator O (in equation (20)). In order for the circuit's output to remain unchanged, this must also change the projected Hilbert spaces of parity measurement of O from $\mathcal{H}_{3A} \otimes \mathcal{H}_{3B}$ to $\mathcal{H}_{2A} \otimes \mathcal{H}_{2B}$, and as a result the unmeasured state is now in $\mathcal{H}_{3A} \otimes \mathcal{H}_{3B}$. The modified \hat{O} is shown to equal \hat{Q}_1 . The Hilbert spaces on which gates in the subsequent Kraus operator \hat{F} act are also swapped between $\mathcal{H}_{3A} \otimes \mathcal{H}_{3B}$ and $\mathcal{H}_{2A} \otimes \mathcal{H}_{2B}$. We then add two other SWAP gates SWAP $_{1A}^{3A}$ SWAP $_{1B}^{3B}$ between the CNOTs and parity measurement of \hat{F} , which changes the parity-measured Hilbert space to $\mathcal{H}_{1A} \otimes \mathcal{H}_{1B}$. This turns \hat{F} into \hat{Q}_2 . We emphasize that the additional SWAP gates are introduced merely for algebraic reasons and are not implemented physically.

As for the term N_2 in equation (32), one can see from the construction of \hat{O}^i and \hat{P}^i (hence \hat{O} and \hat{P}) in equations (20) and (21) that N_2 is essentially N_1 with a swapping of labels of Hilbert spaces $\mathcal{H}_{2A} \otimes \mathcal{H}_{2B}$ and $\mathcal{H}_{1A} \otimes \mathcal{H}_{1B}$. One can then conclude that if the same procedure of addition of SWAP gates are carried out on N_2 , the result will be that on N_1 (in equation (23)) also followed by a relabelling of Hilbert spaces $\mathcal{H}_{2A} \otimes \mathcal{H}_{2B}$ and $\mathcal{H}_{1A} \otimes \mathcal{H}_{1B}$, which is exactly equal to an exchange of \hat{Q}_1 and \hat{Q}_2 , leading to equation (24). The manipulations on M_1 and M_2 follow a similar description that leads to equations (25) and (26). One can see from equations (27) and (28) that \hat{Q}_1 and \hat{Q}_2 are essentially the Kraus operator \hat{O} given in equation (9) but with extra SWAP

gates that relabel the Hilbert spaces of some of the states which do not affect the distillation output. \Box

According to equations (23) and (24), one can regard N_2 as the input state $\rho_{\rm in}$ undergoing trace decreasing maps \hat{Q}_1 and \hat{Q}_2 in the opposite order as that in N_1 . Overall, the circuit in figure 4 before the final Hadamard and parity measurement can be expressed as

$$\rho_s = \hat{W}(\chi_0 \otimes \rho_{\rm in})\hat{W}^{\dagger} + \hat{V}(\chi_0 \otimes \rho_{\rm in})\hat{V}^{\dagger} \tag{35}$$

where

$$\hat{W} = |00\rangle\langle00| \otimes \hat{Q}_2\hat{Q}_1 + |11\rangle\langle11| \otimes \hat{Q}_1\hat{Q}_2 \tag{36}$$

$$\hat{V} = |01\rangle\langle 01| \otimes \hat{J} + |10\rangle\langle 10| \otimes \hat{S}. \tag{37}$$

with \hat{J} and \hat{S} being the operators that act on $\rho_{\rm in}$ in case the control pair is in state $|01\rangle$ and $|10\rangle$. Equation (36) features opposite orders of \hat{Q}_1 and \hat{Q}_2 correlated with different states of the control pair. We have hence shown the circuit in figure 4 simulates two DEJMPS steps applied in a causal order controlled by χ_0 .

C. Explicit Expression of Output State from the Protocol

After the final two Hadamard gates in figure 4, the state in Hilbert space $\mathcal{H}_{0A} \otimes \mathcal{H}_{0B} \otimes \mathcal{H}_{1A} \mathcal{H}_{1B}$ is expressed as

$$\rho_s = \frac{|00\rangle\langle00| + |11\rangle\langle11|}{4} \otimes \rho_+ + \frac{|01\rangle\langle01| + |10\rangle\langle10|}{4} \otimes \rho_- + \rho_{sr}$$
(38)

where

$$\rho_{\pm} = \frac{A_0 + D_0}{2} N_1 + \frac{A_0 + D_0}{2} N_2 + \pm \frac{A_0 - D_0}{2} 2M + \frac{B_0 + C_0}{2} 2T \pm \frac{C_0 - B_0}{2} 2L$$
(39)

and ρ_{sr} consists of off-diagonal elements of the state in $\mathcal{H}_{0A} \otimes \mathcal{H}_{0A}$. Upon parity-measuring χ_0 , ρ_{sr} vanishes. The unmeasured state is post-selected upon an even-parity outcome, making ρ_+ the final product of the protocol

We give explicit expressions of all terms in equation (39) as follows:

$$N_{1} = \begin{pmatrix} A_{1}(A_{2}A_{3} + B_{2}B_{3}) + B_{1}(D_{2}C_{3} + C_{2}D_{3}) \\ D_{1}(C_{2}C_{3} + D_{2}D_{3}) + C_{1}(B_{2}A_{3} + A_{2}B_{3}) \\ C_{1}(C_{2}C_{3} + D_{2}D_{3}) + D_{1}(B_{2}A_{3} + A_{2}B_{3}) \\ B_{1}(A_{2}A_{3} + B_{2}B_{3}) + A_{1}(D_{2}C_{3} + C_{2}D_{3}) \end{pmatrix},$$

$$(40)$$

$$N_{2} = \begin{pmatrix} A_{2}(A_{1}A_{3} + B_{1}B_{3}) + B_{2}(D_{1}C_{3} + C_{1}D_{3}) \\ D_{2}(C_{1}C_{3} + D_{1}D_{3}) + C_{2}(B_{1}A_{3} + A_{1}B_{3}) \\ C_{2}(C_{1}C_{3} + D_{1}D_{3}) + D_{2}(B_{1}A_{3} + A_{1}B_{3}) \\ B_{2}(A_{1}A_{3} + B_{1}B_{3}) + A_{2}(D_{1}C_{3} + C_{1}D_{3}) \end{pmatrix},$$

$$(41)$$

$$M_1 = M_2 = \begin{pmatrix} A_3 A_2 A_1 \\ B_3 B_2 B_1 \\ C_3 C_2 C_1 \\ D_3 D_2 D_1 \end{pmatrix}. \tag{42}$$

 T_1 , T_2 and L are expressed as

$$T_{1} = T_{2} = \frac{1}{4} \begin{pmatrix} \sum_{a,b,c,d=0}^{1} m_{a,b}^{(1)} m_{c,d}^{(2)} m_{a \oplus c,b \oplus d}^{(3)} \\ \sum_{a,b,c,d=0}^{1} m_{a,b}^{(1)} m_{c,d}^{(2)} m_{a \oplus c \oplus 1,b \oplus d \oplus 1}^{(3)} \\ \sum_{a,b,c,d=0}^{1} m_{a,b}^{(1)} m_{c,d}^{(2)} m_{a \oplus c \oplus 1,b \oplus d}^{(3)} \\ \sum_{a,b,c,d=0}^{1} m_{a,b}^{(1)} m_{c,d}^{(2)} m_{a \oplus c,b \oplus d \oplus 1}^{(3)} \end{pmatrix}, (43)$$

$$L = \frac{1}{4} \begin{pmatrix} \sum_{\substack{a,b,\\c,d=0}}^{1} m_{a,b}^{(1)} m_{c,d}^{(2)} m_{a\oplus c,b\oplus d}^{(3)} (-1)^{a(1\oplus d)\oplus c(1\oplus b)} \\ \sum_{\substack{c,d=0\\c,d=0}}^{1} m_{a,b}^{(1)} m_{c,d}^{(2)} m_{a\oplus c\oplus 1,b\oplus d\oplus 1}^{(3)} (-1)^{(a\oplus 1)d\oplus (c\oplus 1)b} \\ \sum_{\substack{a,b,\\c,d=0}}^{1} m_{a,b}^{(1)} m_{c,d}^{(2)} m_{a\oplus c\oplus 1,b\oplus d}^{(3)} (-1)^{a(1\oplus d)\oplus c(1\oplus b)\oplus b\oplus d} \\ \sum_{\substack{c,d=0\\c,d=0}}^{1} m_{a,b}^{(1)} m_{c,d}^{(2)} m_{a\oplus c\oplus 1,b\oplus d}^{(3)} (-1)^{a(1\oplus d)\oplus c(1\oplus b)\oplus b\oplus d} \end{pmatrix}. \quad (44)$$

In equations (43) and (44), the definition of $m_{j,k}^{(i)}$ was given in equation (29). \oplus is binary addition acting on $a,b \in \{0,1\}$ such that $a \oplus b = \text{mod}(a+b,2)$.

V. ADVANTAGE IN FIDELITY AND PROBABILITY OF SUCCESS

In previous works, the advantage of indefinite causal structures were argued via comparison with definite causal structures that consist of the same number of quantum operations. Similarly for our set of protocols \mathcal{S} , a comparison with conventional concatenation of two DEJMPS steps suffices to show the advantage of indefinite causal order. But here in \mathcal{S} , the control of causal order is carried out by a fourth faulty entangled pair. From the point of view of the task of entanglement distillation, this entangled pair is seen as extra resource. We therefore must compare \mathcal{S} with definite-causal-order

protocols that also turn four faulty entangled pairs into one. These protocols are exactly those that form the set of protocols $\mathcal G$ as defined in section III A, which consist of up to *three* DEJMPS steps.

The most important metrics of two-way entanglement distillation protocols are the fidelity of distillation and probability of success. We note that the output of the protocol ρ_{+} from equation (39) is a mixture of five terms: N_1, N_2, M, T and L (where we can express M as $M = \frac{1}{2}(N_1 + N_2 + [\hat{Q}_2, \hat{Q}_1]\rho_{\rm in}[\hat{Q}_2, \hat{Q}_1])$. In order for ρ_+ to have a fidelity advantage over the distillation products of all protocols in \mathcal{G} , at least one term among M, T and L must have a fidelity larger than both N_1 and N_2 , since N_1 and N_2 themselves are the product of distillation from two definite-ordered DEJMPS steps, which are member protocols of the set \mathcal{G} . In this section, aside from comparing the fidelities and probabilities of success of protocol set S and G, we present that the advantage in fidelity solely comes from M (rather than from T and L), owing to the non-trivial commutation (i.e. $[\hat{Q}_2, \hat{Q}_1] \neq 0$) between the Kraus operators of the two maps that describe the two DEJMPS steps. This is the same origin as that of the advantage of a quantum switch as reviewed earlier in section II. This confirms that the advantage in fidelity of our scheme is indeed due to applying entanglement distillation maps in a coherent superposition of two causal orders.

We first present some discrete examples of input states χ_i where protocol set \mathcal{S} returns a higher fidelity than protocols in \mathcal{G} . We also find that for some of these examples they also result in higher success probability, showing clear advantage of protocols \mathcal{S} . We then seek to compare the two set of protocols using a single metric which takes into account both the fidelity and success probability. We achieve this by setting up an amalgamated entanglement distillation scheme which has one extra DEJMPS step after the initial protocol and analyse its final fidelity.

A. Discrete Advantageous Input Examples

1. Werner States as Input

An infinite number of examples actually exist since there is a continuous region of input state parameters where the advantage holds. Here we begin with presenting discrete examples to show their existence. We first consider the case when they are all Werner states of the form $\chi_i = F_i |\Phi^+\rangle\langle\Phi^+| + (1 F_i$)/3($|\Psi^-\rangle\langle\Psi^-| + |\Psi^+\rangle\langle\Psi^+| + |\Phi^-\rangle\langle\Phi^-|$) and search over the parameter space $\mathbf{F} = [F_0, F_1, F_2, F_3]$. For a set of parameters \mathbf{F} , we find, over all protocols in \mathcal{S} , the one that gives the maximum fidelity F_S and also find its probability of success p_S . Then we find, for the same \mathbf{F} , the maximum fidelity $F_{\mathcal{G}}$ among all protocols in \mathcal{G} and calculate its success probability $p_{\mathcal{G}}$. A search using the basinhopping algorithm [32] that minimises $F_{\mathcal{G}} - F_{\mathcal{S}}$ over the parameter space yields $\mathbf{F} = [0.5390, 0.6348, 0.6348, 0.5891]$. When the four input states have those parameters, the set of protocols \mathcal{S} produce a state $\rho_+ = (0.6870, 0.0797, 0.0797, 0.1536)^{\mathrm{T}}$ with fidelity $F_{\mathcal{S}} = 0.6870$ and $p_{\mathcal{S}} = 0.2126$. Among all the protocols in \mathcal{G} , the one with a recurrence-like structure first combining χ_0 with χ_2 and χ_1 with χ_3 before combining their purified products yields a state $(0.6858, 0.0549, 0.1309, 0.1285)^{\mathrm{T}}$ with $p_{\mathcal{G}} = 0.2074$. Our set of protocols \mathcal{S} has a fidelity advantage $F_{\mathcal{S}} - F_{\mathcal{G}} = 0.0012$ and a success probability advantage $p_{\mathcal{S}} - p_{\mathcal{G}} = 0.0052$ over protocols \mathcal{G} . This shows clear overall advantage of the protocol set \mathcal{S} .

As presented in equation (39), ρ_{+} is a weighted mixture of N_1 , N_2 , M, T and L, each of which being an unormalized mixture of the four Bell states. We calculate the fidelities of all the mixture components of ρ_{+} and they are: $f(N_1) = f(N_2) = 0.6858$, f(M) = 0.9750, f(T) = 0.3393, f(L) = 0.6304. M is the only component with a fidelity higher than N_1 and N_2 , which are the fidelities of the entangled state produced from doing two definite-ordered DEJMPS steps. This means the fidelity advantage of protocols \mathcal{S} is solely due to the presence of the component M. As discussed in section IV, the presence of M is due to the non-trivial commutations of the Kraus operators that correspond to the maps of the two distillation steps. This shows that the fidelity advantage of protocols S indeed comes from two DEJMPS steps being applied in an indefinite causal order.

2. General Bell-diagonal States as Input

We also relax the Werner state assumption to allow χ_i s to have general Bell-diagonal shape. In this case, the basinhopping optimization seeks to minimise $F_{\mathcal{G}} - F_{\mathcal{S}}$ over a much larger parameter space. The algorithm yields $\chi_0 = (0.7860, 0.2140, 0, 0)^{\mathrm{T}}, \ \chi_1 = (0.7938, 0.2062, 0, 0)^{\mathrm{T}}, \ \chi_2 = (0.7926, 0.2074, 0, 0)^{\mathrm{T}}, \ \chi_3 = (0.7156, 0.2174, 0, 0)^{\mathrm{T}}.$ Protocols S now gives $\rho_{+} = (0.8707, 0.0022, 0, 0.1265)^{T}$ with success probability $p_{\mathcal{S}} = 0.4225$. Among protocols in \mathcal{G} , the one with a recurrence-like structure first combining (χ_0, χ_3) and (χ_1, χ_2) then combining the respective distillation products yields $(0.7938, 0, 0.2062, 0)^{\mathrm{T}}$ with probability 0.5155. Our scheme has a much higher fidelity (by $F_S - F_G = 0.8707 - 0.7938 \approx 0.08$), which outweighs the slight disadvantage in success probabil-Here, the different mixture components of ρ_+ have the following fidelities: $f(N_1) = 0.7860, f(N_2) =$ 0.7938, f(M) = 0.9818, f(T) = f(L) = 0.5983. Again, M is the only component with a fidelity higher than N_1 and N_2 , showing the fidelity advantage over definiteordered concatenation of steps is solely due to M.

B. Advantageous Region of Parameters

We now would like to compare the two sets of protocols using a single metric which takes into account both the

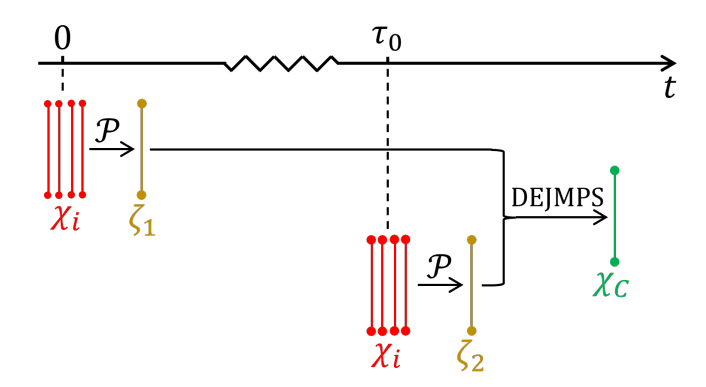


FIG. 5. An amalgamated entanglement distillation scheme which consists of protocol \mathcal{P} (selected from set of protocols \mathcal{S} or \mathcal{G}) followed by a DEJMPS distillation step. The scheme turns eight faulty entangled pairs, which consists of two batches of four pairs, into one. χ_i , $\zeta_{1(2)}$ and χ_C denote the entangled pairs before protocol \mathcal{P} , after \mathcal{P} and after the final DEJMPS step. τ_0 : time interval between supplies of two batches of faulty pairs.

fidelity of the product and probability of success. This is achieved by considering the following communication scenario. Suppose the four faulty pairs χ_i s were generated at the same time in a batch and they all experienced the same noise which has the following shape:

$$\chi_i = \left(F, (1-F)r, (1-F)(\frac{1-r}{2}), (1-F)(\frac{1-r}{2})\right)^{\mathrm{T}}$$
(45)

where we term r the "noise bias" of χ_i (To keep the discussion simple, we add a simple bias on top of the generic depolarising noise and refrain from analysing noise with an arbitrary shape). Upon generation, the entangled pairs are subject to immediate distillation under a protocol $\mathcal{P} \in \mathcal{G}$ or \mathcal{S} . In general, the requested fidelity from the user of the entangled pairs can be much higher than that of the original supply, which warrants further entanglement distillation after an initial distillation effort. We therefore introduce the following amalgamated distillation scheme: after an initial distillation using the protocol \mathcal{P} , the distilled product, denoted as ζ_1 , is stored in the repeaters to wait to undergo one further DEJMPS step with the distilled product of \mathcal{P} from the next batch of four entangled pairs, denoted as ζ_2 . We denote the product after the final DEJMPS step as χ_C . The amalgamated scheme is also illustrated in figure 5. While ζ_1 is waiting for ζ_2 to be generated, it is stored in quantum memories. We assume the memories have a depolarising noise of the following form:

$$\hat{\chi}_i \to \hat{\chi}_i(t) = e^{-\lambda t} \hat{\chi}_{it=0} + \frac{1 - e^{-\lambda t}}{4} \mathbb{1}$$
 (46)

where t is the temporal length of storage, λ is the decay rate of the register and 1 is the identity matrix. The fidelity of ζ_1 degrades as it waits for ζ_2 for the final DE-JMPS step. The time of waiting is directly influenced

by the success probability of \mathcal{P} . The fidelity of the final product, $f(\chi_C)$, is hence a function of both the fidelity and success probability of \mathcal{P} . The probabilistic nature of \mathcal{P} will make $f(\chi_C)$ follow a distribution which has a mean value denoted as \bar{F} (In fact, ζ_2 may come in so late that ζ_1 has degraded so much, rendering the final distillation step useless, in which case ζ_1 is simply discarded, making $\chi_C = \zeta_2$). We use \bar{F} , which is a function of λ , F and r, as our metric to compare the two sets of protocols \mathcal{G} and \mathcal{S} .

For a given F, r and λ , we calculate the maximum \bar{F} for all $\mathcal{P} \in \mathcal{S}$ which we denote as $\bar{F}_{\mathcal{S}}$, and the maximum \bar{F} for all $\mathcal{P} \in \mathcal{G}$ denoted as $\bar{F}_{\mathcal{G}}$. We want to find out the regions of parameters where $\bar{F}_{\mathcal{S}} > \bar{F}_{\mathcal{G}}$, that is, under what kind of noise of entanglement generation (characterised by F and r) and what level of storage noise (characterised by λ) does using the set of protocols \mathcal{S} in the amalgamated distillation scheme give a higher fidelity of the final distilled pair? We also assume rate of entanglement generation is small so that the time taken to complete the protocol \mathcal{P} is much shorter than τ_0 , the time interval between generation of two consecutive batches of entangled pairs.

The contours where $\bar{F}_{\mathcal{S}} = \bar{F}_{\mathcal{G}}$ for several different supplied fidelities F under different λ and r are shown in figure 6. For each curve in figure 6, the region on the left hand side of the curve has $\bar{F}_{\mathcal{S}} < \bar{F}_{\mathcal{G}}$, and the region on the right hand side of each curve has $\bar{F}_{\mathcal{S}} > \bar{F}_{\mathcal{G}}$ where our modified protocols \mathcal{S} has advantage. Here we discuss several features of the graph. The advantageous region is larger for lower F and smaller for higher F. For each F, advantage of our scheme is seen under large r, when the noise on each χ_i is highly biased towards Pauli-Y, and has no advantage under small r, when the noise is biased away from Pauli-Y. In particular, no advantage is seen under any λ for four identical Werner states (marked by a dashed line, where r=1/3), despite we have shown in section VA1 the existence of advantage for certain combinations of Werner states of distinct fidelities. For each F, the $\bar{F}_{\mathcal{S}} = \bar{F}_{\mathcal{G}}$ boundary shows a generally negative correlation between λ and r. We interpret this with an example of input state χ_i at $F=0.7,\,r=0.59$ and zero storage noise at $\lambda = 0$. One can show that the fidelities after the first distillation step from the two set of protocols actually have $f(\zeta_2(\mathcal{P} \in \mathcal{S})) > f(\zeta_2(\mathcal{P} \in \mathcal{G}))$. However, after the final DEJMPS step, $\bar{F}_{S} < \bar{F}_{G}$, as one can see from figure 6 that the data point $(r = 0.59, \lambda = 0)$ lies on the left hand side of the curve F = 0.7. This is due to that $\zeta_2(\mathcal{P} \in \mathcal{S})$ has a shape less favourable for the final DEJMPS step than $\zeta_2(\mathcal{P} \in \mathcal{G})$. On the other hand, in the limit of high memory noise (large λ), the final DEJMPS step is useless. In this case, the distillation product after the first step is simply kept as final output: $\chi_C = \zeta_2$, making $\bar{F}_S = f(\zeta_2(S)) > \bar{F}_G = f(\zeta_2(G))$. Therefore there must be some λ in between where $\bar{F}_S = \bar{F}_G$.

To make our model of the practical situation more realistic, We introduce a diffusion of arrival times of the four entangled pairs in the same batch. Consider τ , the time

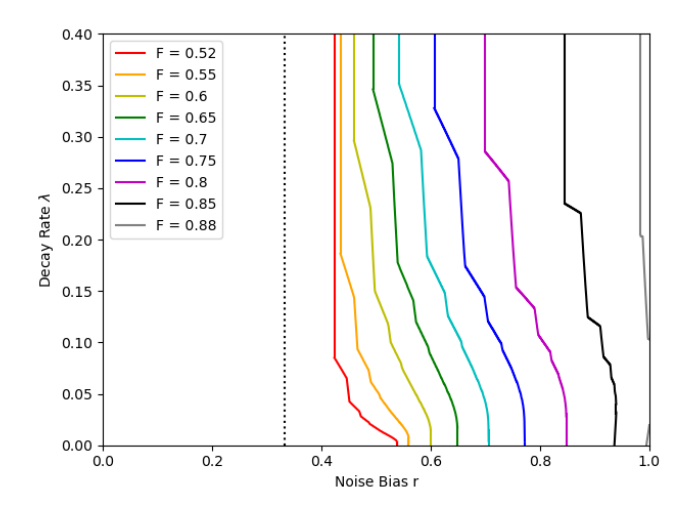


FIG. 6. Each curve in the figure specifies a certain fidelity F of input states. On the *right hand side* of a curve are the set of parameters (r, λ) (along with the given fidelity F) that result in the amalgamated distillation scheme giving $\bar{F}_S > \bar{F}_{\mathcal{G}}$, where our set of protocols \mathcal{S} show advantage. On the *left hand side* of the curve are the set of parameters that result in $\bar{F}_S < \bar{F}_{\mathcal{G}}$, where the definite-causal-order protocols \mathcal{G} show advantage. Exactly *along* the curves are the set of parameters that give $\bar{F}_S = \bar{F}_{\mathcal{G}}$. The vertical dotted line has r = 1/3 where the input states are Werner states.

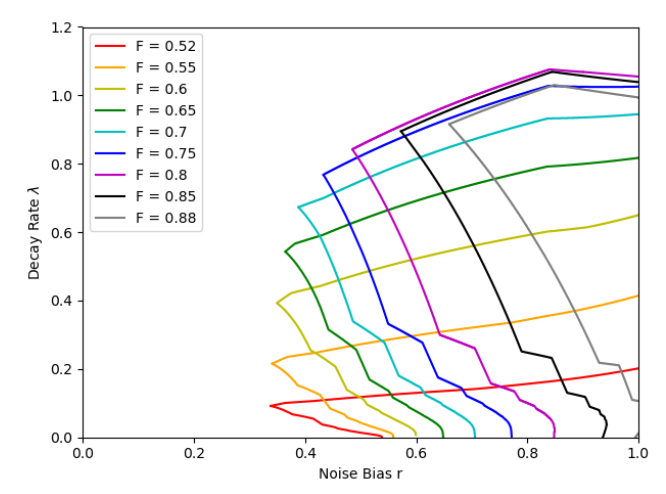


FIG. 7. Contours of $\bar{F}_S = \bar{F}_{\mathcal{G}}$ when the difference of moments of arrival of the first and last of the four pairs in a batch is $0.5\tau_0$, where τ_0 is the time interval between consecutive arrivals of two *batches*.

difference of first and last arrivals of the four as $\tau=0.5\tau_0$, and any two consecutive arrivals are equally separated in time by $0.5\tau_0/3$. Distillation protocol \mathcal{P} is applied only after the last of the four pairs arrive, when the earlier-arrived pairs will have degraded. We re-calculate $\bar{F}_{\mathcal{S}}$ and $\bar{F}_{\mathcal{G}}$ and show the contours where $\bar{F}_{\mathcal{S}} = \bar{F}_{\mathcal{G}}$ in figure 7. Figure 7 has two main features different from figure 6. First, the advantageous region where $\bar{F}_{\mathcal{S}} > \bar{F}_{\mathcal{G}}$ of each F expands to smaller values of r than that in figure 6. This

is somewhat expected since difference in arrival times of each pair results in different fidelities of the four pairs on which protocol $\mathcal P$ is applied due to storage noise, and as discussed earlier, some advantage is seen for unequal Werner states while no advantage is seen for distinct Werner states. Second, the advantageous region for each F closes at some decay rate. This is because when λ is large, the earlier arrived faulty pairs will have degraded to having fidelities lower than 0.5, making them useless for distillation, but the later arrived pairs can still be purified, so the protocols in $\mathcal G$ necessarily perform better at large λ than our protocols in $\mathcal S$, which require no fewer than four pairs to operate.

VI. CONCLUSION

We have shown that applying two steps of DEJMPS distillation protocol in a superposition of causal orders, for some parameters of the input faulty pairs, results in higher distillation fidelity and probability of success than applying steps of the protocol in a definite causal order. We have also shown the overall trace-decreasing map the input faulty states go through can be expressed in the same form as a quantum switch, which indicates the presence of indefinite orders of two trace-decreasing maps. In contrast to previous scenarios of indefinite causal order where the proposed application setting is purely theoretical, our proposal is an example of advantageous application of indefinite causal order in a practical situation of quantum communication. The circuit of our scheme has relatively low complexity, making the protocol viable to implement and demonstrate experimentally. As discussed in section V, our protocol has large fidelity advantage when noise on the faulty pairs is highly biased, making itself useful in many practical situations, where biased noise is ubiquitous.

Our results open up the following directions for future work. A natural and immediate extension is to analyze the advantage of fidelity and success probability of applying m > 2 DEJMPS steps in an indefinite causal order over those of definite-ordered concatenations of up to m+1 steps. Extensions to studying other two-way distillation protocols with different initial rotations [33] (instead of $\hat{R} = \exp(-\frac{i\pi}{2}\hat{X})$ in DEJMPS's protocol), multipartite entanglement distillation protocols [34] and oneway entanglement distillation protocols [35] can be carried out. Given the known connection [21] of one-way entanglement distillation protocols with stabilizer quantum error correction codes, we hope the possible existence of such advantages can stimulate effort into incorporating indefinite causal structures into the encoding/decoding of quantum error correction codes, which is a vital part of practical quantum computation and quantum communication.

We point out that modifications similar to our proposal can be envisioned for many other distillation-like and breeding-like protocols that feature repeated appli-

cations of some subroutine, each featuring a subsystem interacting with ancillary states. This includes, but of course not limited to, the following examples: distillation of magic states for universal quantum computation [36, 37], and repeated breeding of oscillator states [38] for inter-conversion of bosonic quantum error-correction codes. For the above examples, control-swaps of supplied imperfect states can be carried out. The natural question would be to determine, for each task, the fidelities and production yields of the output states. A higher fidelity/production yield can mean a reduction in the overhead of the task [37], which benefits practical quantum computation.

ACKNOWLEDGMENTS

We acknowledge financial supports from Imperial College London through the Presidential Scholarship, the EPSRC through EP/T00097X/1 and EP/T001062/1 and the Korean Institute of Science and Technology for their Open Innovation Lab programme.

Appendix A: Two Quantum Teleportation Steps Applied under Indefinite Causal Order

One noticeable proposal for application of indefinite causal order in quantum communication is putting two teleportation steps in a superposition of causal order. The standard quantum teleportation protocol [39] has a $|\Phi^+\rangle$ state shared between Alice and Bob. For Alice to teleport her qubit $|\psi\rangle$, she performs a Bell measurement between $|\psi\rangle$ and her qubit of $|\Phi^+\rangle$. The measurement result is sent to Bob via a classical channel. Bob maps the measurement result onto a Pauli operator which he performs on the teleported state to recover $|\psi\rangle$. It is known from [40] that when the shared entangled state is noisy, the above protocol is essentially $|\psi\rangle$ undergoing a generalized depolarising channel. Two noisy teleportation steps applied in series naturally degrades $|\psi\rangle$ more

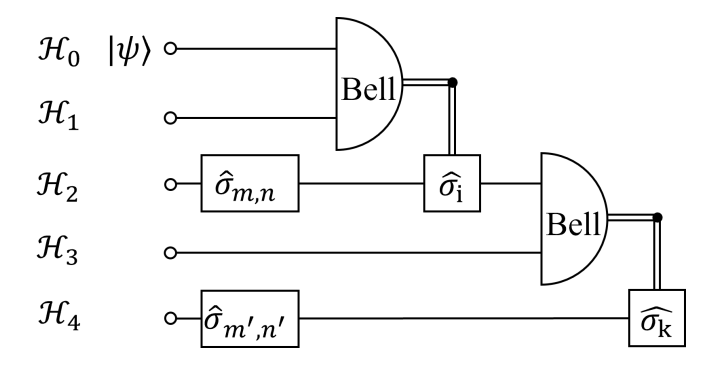


FIG. 8. Circuit for two concatenated steps of noisy teleportation. \mathcal{H}_i where $i \in \{0, 1, 2, 3, 4\}$ denotes the Hilbert spaces of the corresponding qubits.

than one step. It was claimed, however, in [17, 19] and [18] that applying two teleportation steps in an indefinite causal order reduces can the noise of the final target state as compared to the two steps applied back-to-back. In [18], a photonic implementation of this scheme is proposed where entangled photon pairs pass through beam splitters and subsequent Bell measurements such that a distinct causal order is featured on each output path of the beam splitters. On one of the two paths, SWAP gates are performed on the photon pairs to simulate the swapping of teleportation channels. The author in [18] considered the case when the entangled pair is pure but not maximally entangled. In this section we examine their proposals [17–19] more carefully and show that no noise reduction of the target state actually occurs.

We first consider two concatenated standard teleportation steps with the input target state $|\psi\rangle\langle\psi|$ in Hilbert space \mathcal{H}_0 , whose circuit in shown in figure 8. A pure but not maximally entangled state χ is in Hilbert space $\mathcal{H}_1 \otimes \mathcal{H}_2$:

$$\chi = \sum_{mn} \sigma_m^{(2)} |\Phi^+\rangle \langle \Phi^+| \sigma_n^{(2)} q_{mn}$$
 (A1)

where σ_m and σ_n are Pauli operators, the superscript "2" means the Pauli noise occurs on the qubit of χ in Hilbert space \mathcal{H}_2 as denoted in figure 8. q_{mn} denotes the entries of the density matrix under the Bell basis. A second pure yet not maximally entangled pair ξ lies in Hilbert space $\mathcal{H}_3 \otimes \mathcal{H}_4$:

$$\xi = \sum_{m'n'} \sigma_{m'}^{(4)} |\Phi^{+}\rangle \langle \Phi^{+} | \sigma_{n'}^{(4)} s_{m'n'}. \tag{A2}$$

The superscripts "4" again denotes the Hilbert space on which we assume Pauli noise occurs. The first teleportation step carried out with χ and the original target state $|\psi\rangle\langle\psi|$ yields

$$\rho = \sum_{nmi} \sigma_i^{(2)} G_i^{(01)} |\psi\rangle\langle\psi| \otimes \sigma_n^{(2)} |\Phi^+\rangle\langle\Phi^+| \sigma_m^{(2)} q_{mn} G_i^{(01)} \sigma_i^{(2)}$$
(A3)

where $G_i^{(01)}$ is the Bell measurement projector associated with outcome i and $\sigma_i^{(2)}$ is the corresponding Pauli correction applied on the output Hilbert space. We now want to express the errors on ρ in terms of the errors σ_m, σ_n on χ . The Pauli errors σ_n and σ_m commute with $G_i^{(01)}$ as they act on different Hilbert spaces. They commute with σ_i if m(n) = i, or anti-commute with σ_i if otherwise. This means

$$\rho = \sum_{nmi} \sigma_n^{(2)} \left(\sigma_i^{(2)} G_i^{(01)} |\psi\rangle \langle \psi| \otimes |\Phi^+\rangle \langle \Phi^+| G_i^{(01)} \sigma_i^{(2)} \right)$$

$$\sigma_m^{(2)} A_{ni} A_{im} q_{mn}$$

$$= \sum_{nmi} \sigma_n^{(2)} |\psi\rangle \langle \psi| \sigma_m^{(2)} A_{ni} A_{im} q_{mn}$$
(A4)

where A is a global phase caused by permuting $\sigma_{m,n}$ with σ_i . $A_{ni} = 1$ when $[\sigma_n, \sigma_i] = 0$ and = -1 if they

anti-commute. The second line is due to the part in the large parenthesis is simply $|\psi\rangle\langle\psi|$ which comes from a perfect teleportation with noiseless $|\Phi^+\rangle$. We note that $\sum_i A_{ni} A_{im} = \delta_{nm}$. This eliminates all summing components where $n \neq m$ and we arrive at

$$\rho = \sum_{m} \sigma_{m} |\psi\rangle\langle\psi|\sigma_{m} q_{mm} \tag{A5}$$

which, as expected from [40], is the original state $|\psi\rangle$ undergone a depolarising channel. ρ now goes through the second teleportation channel which has an output ρ' expressed as

$$\rho' = \sum_{mm'n'k} \sigma_k^{(4)} G_k^{(23)} [\sigma_m^{(2)} | \psi \rangle \langle \psi | \sigma_m^{(2)} q_{mn}] \otimes$$

$$\sigma_{m'}^{(4)} | \Phi^+ \rangle \langle \Phi^+ | \sigma_{n'}^{(4)} s_{m'n'} G_k^{(23)} \sigma_k^{(4)}$$
(A6)

where the superscripts denote the Hilbert spaces of the corresponding operations. Like before, we move $\sigma_{m'}^{(4)}$ and $\sigma_{n'}^{(4)}$ across the Pauli corrections during which global phases $A_{m'k}$ and $A_{n'k}$ arise:

$$\rho' = \sum_{mm'n'k} \sigma_{m'}^{(4)} \sigma_k^{(4)} G_k^{(23)} [\sigma_m^{(2)} | \psi \rangle \langle \psi | \sigma_m^{(2)} q_{mn}] \otimes |\Phi^+\rangle \langle \Phi^+ | s_{m'n'} G_k^{(23)} \sigma_k^{(4)} \sigma_{n'}^{(4)} A_{m'k} A_{n'k}.$$

We notice that ρ now can be interpreted as the inner state $\sigma_m^{(2)}|\psi\rangle\langle\psi|\sigma_m^{(2)}$ passing through a perfect teleportation channel followed by $\sigma_{m'}^{(4)}$ on the ket side (or $\sigma_{n'}^{(4)}$ on the bra side). Since a perfect teleportation preserves the target state, a Pauli error $\sigma_m^{(2)}$ commutes with a perfect teleportation. Having an error on the input target state has the same effect as having the error on the perfectly teleported state. We can hence move $\sigma_m^{(2)}$ across $\sigma_k^{(4)}$ and $G_k^{(23)}$, giving

$$\rho' = \sum_{mm'n'k} \sigma_{m'}^{(4)} \sigma_{m}^{(4)} [\sigma_{k}^{(4)} G_{k}^{(23)} | \psi \rangle \langle \psi | \otimes | \Phi^{+} \rangle \langle \Phi^{+} | G_{k}^{(23)} \sigma_{k}^{(4)}]$$

$$\sigma_{m}^{(4)} \sigma_{n'}^{(4)} A_{m'k} A_{n'k} q_{mn} s_{m'n'}$$

$$= \sum_{mm'n'k} \sigma_{m'}^{(4)} \sigma_{m}^{(4)} | \psi \rangle \langle \psi | \sigma_{m}^{(4)} \sigma_{n'}^{(4)} A_{m'k} A_{n'k} q_{mn} s_{m'n'}$$

$$= \sum_{mm'n'k} \sigma_{m'}^{(4)} \sigma_{m}^{(4)} | \psi \rangle \langle \psi | \sigma_{m}^{(4)} \sigma_{n'}^{(4)} \delta_{m'n'} q_{mn} s_{m'n'}$$

$$= \sum_{mn} \sigma_{n} \sigma_{m} | \psi \rangle \langle \psi | \sigma_{m} \sigma_{n} q_{mm} s_{nn}$$
(A8)

We now calculate the state produced from the scheme proposed in [18] which uses a control qubit $|c\rangle = |+\rangle = 1/\sqrt{2}(|0\rangle + |1\rangle)$ to swap χ and ξ , then does the two teleportation steps before measuring $|c\rangle$ in the Fourier basis and post-selecting the "+" outcome. Before measuring $|c\rangle$, the overall state \hat{R} which consists of $|c\rangle$ and telepor-

tation target state $|\psi\rangle$ reads

$$\begin{split} R = & \frac{|0\rangle\langle 0|}{2} \otimes \sum_{mn} \sigma_{n} \sigma_{m} |\psi\rangle\langle \psi| \sigma_{m} \sigma_{n} q_{mm} s_{nn} \\ & + \frac{|1\rangle\langle 1|}{2} \otimes \sum_{mn} \sigma_{m} \sigma_{n} |\psi\rangle\langle \psi| \sigma_{n} \sigma_{m} q_{mm} s_{nn} \\ & + \frac{|0\rangle\langle 1|}{2} \otimes \sum_{mnm'n'ik} \sigma_{k}^{(4)} G_{k}^{(23)} [\sigma_{i}^{(2)} G_{i}^{(01)} |\psi\rangle\langle \psi| \otimes \\ & \sigma_{m}^{(2)} |\Phi^{+}\rangle\langle \Phi^{+} |\sigma_{n'}^{(2)} q_{mn} G_{i}^{(01)} \sigma_{i}^{(2)}] \otimes \sigma_{m'}^{(4)} |\Phi^{+}\rangle\langle \Phi^{+} |\sigma_{n}^{(2)} s_{m'n'} G_{k}^{(23)} \sigma_{k}^{(4)} \\ & + \frac{|1\rangle\langle 0|}{2} \otimes \sum_{mnm'n'ik} \sigma_{k}^{(4)} G_{k}^{(23)} [\sigma_{i}^{(2)} G_{i}^{(01)} |\psi\rangle\langle \psi| \otimes \\ & \sigma_{m'}^{(2)} |\Phi^{+}\rangle\langle \Phi^{+} |\sigma_{n}^{(2)} q_{mn} G_{i}^{(01)} \sigma_{i}^{(2)}] \otimes \sigma_{m}^{(4)} |\Phi^{+}\rangle\langle \Phi^{+} |\sigma_{n'}^{(2)} s_{m'n'} G_{k}^{(23)} \sigma_{k}^{(4)}. \end{split}$$

For the last two terms in the summation, we follow a similar strategy by moving the Pauli errors on the entangled pairs pass the Pauli corrections where global phases arise from commutation (or anti-commutation). This gives

$$R = \frac{|0\rangle\langle 0|}{2} \otimes \sum_{mn} \sigma_{n} \sigma_{m} |\psi\rangle\langle \psi| \sigma_{m} \sigma_{n} q_{mm} s_{nn}$$

$$+ \frac{|1\rangle\langle 1|}{2} \otimes \sum_{mn} \sigma_{m} \sigma_{n} |\psi\rangle\langle \psi| \sigma_{n} \sigma_{m} q_{mm} s_{nn}$$

$$+ \frac{|0\rangle\langle 1|}{2} \otimes \sum_{mn} \sigma_{n} \sigma_{m} |\psi\rangle\langle \psi| \sigma_{m} \sigma_{n} q_{mn} s_{nm}$$

$$+ \frac{|1\rangle\langle 0|}{2} \otimes \sum_{mn} \sigma_{m} \sigma_{n} |\psi\rangle\langle \psi| \sigma_{n} \sigma_{m} q_{mn} s_{nm}$$

$$+ \frac{|1\rangle\langle 0|}{2} \otimes \sum_{mn} \sigma_{m} \sigma_{n} |\psi\rangle\langle \psi| \sigma_{n} \sigma_{m} q_{mn} s_{nm}$$
(A10)

The fact that χ and ξ are pure states means that s_{mn} and q_{mn} are factorizable: they can be written as $s_{mn} = u_m u_n^*$

and $q_{mn}=v_mv_n^*$ where $\mathbf{u}=\{u_m\}$ and $\mathbf{v}=\{v_m\}$ are normalized probability amplitudes of each Bell component such that $|\mathbf{u}|=|\mathbf{v}|=1$. We consider a common situation (which is also the case considered in [18]) where the two faulty pairs, χ and ξ , are identical. This is motivated from the speculation that they may come from the same single photon generator. This means $\mathbf{u}=\mathbf{v}e^{i\phi}$ with some constant phase factor ϕ . We then have $q_{mn}s_{nm}=v_mv_n^*u_nu_m^*=v_m(u_n^*e^{i\phi})u_n(v_m^*e^{-i\phi})=v_mv_m^*u_nu_n^*=q_{mm}s_{nn}$. Substituting this into equation (A10) and notice that $\sigma_n\sigma_m|\psi\rangle\langle\psi|\sigma_m\sigma_n=\sigma_m\sigma_n|\psi\rangle\langle\psi|\sigma_n\sigma_m$ for any n,m since σ_n and σ_m either commute or anti-commute, one can express \hat{R} as

$$R = |+\rangle\langle +| \otimes \rho' \tag{A11}$$

which yields an output state ρ' , the same as that from two definite-order teleportation steps, regardless of the basis and outcome of measurement on the control qubit. no noise reduction has occurred.

We leave as future work to examine the more general case when χ and ξ are mixed states. We expect, however, more practical challenges to implement the scheme in [18] in this case. This is because the mixed Pauli noise is likely to occur during storage or transmission of the entangled states. It is not hard to see that in order for noise interference to occur due to indefinite causal order. controlled-swapping of the two entangled pairs must happen after, not before the mixed Pauli noises. This means if, for example, the major source of noise comes from the physical communication channel during transmissions of the entangled pairs, the controlled-swap will have to be carried out between remote parties. Suppose the two faulty entangled pairs are shared between Alice & Bob and Bob & Charlie, respectively, then extra perfect Bell pairs will have to be pre-shared between Alice & Charlie for the remote-swap. The required extra resources bring additional challenges to the practical implementation.

O. Oreshkov, F. Costa, and Č. Brukner, Nature Communications 3, 1092 (2012).

^[2] T. Colnaghi, G. M. D'Ariano, S. Facchini, and P. Perinotti, Physics Letters A 376, 2940 (2012).

^[3] G. Chiribella, G. M. D'Ariano, P. Perinotti, and B. Valiron, Phys. Rev. A 88, 022318 (2013).

^[4] M. Araújo, F. Costa, and Č. Brukner, Phys. Rev. Lett. 113, 250402 (2014).

^[5] M. J. Renner and Č. Brukner, Phys. Rev. Res. 3, 043012 (2021).

^[6] M. M. Taddei, J. Cariñe, D. Martínez, T. García, N. Guerrero, A. A. Abbott, M. Araújo, C. Branciard, E. S. Gómez, S. P. Walborn, L. Aolita, and G. Lima, PRX Quantum 2, 010320 (2021).

^[7] M. J. Renner and Č. Brukner, Phys. Rev. Lett. 128, 230503 (2022).

^[8] A. Feix, M. Araújo, and Č. Brukner, Phys. Rev. A 92, 052326 (2015).

^[9] P. A. Guérin, A. Feix, M. Araújo, and Č. Brukner, Phys. Rev. Lett. 117, 100502 (2016).

^[10] D. Ebler, S. Salek, and G. Chiribella, Phys. Rev. Lett. 120, 120502 (2018).

^[11] G. Chiribella, M. Banik, S. S. Bhattacharya, T. Guha, M. Alimuddin, A. Roy, S. Saha, S. Agrawal, and G. Kar, New Journal of Physics 23, 033039 (2021).

^[12] L. M. Procopio, F. Delgado, M. Enríquez, N. Belabas, and J. A. Levenson, Entropy 21, 1012 (2019).

^[13] L. M. Procopio, F. Delgado, M. Enríquez, N. Belabas, and J. A. Levenson, Phys. Rev. A 101, 012346 (2020).

^[14] M. Caleffi and A. S. Cacciapuoti, IEEE Journal on Selected Areas in Communications 38, 575 (2020).

^[15] S. S. Bhattacharya, A. G. Maity, T. Guha, G. Chiribella, and M. Banik, PRX Quantum 2, 020350 (2021).

^[16] J. Wechs, H. Dourdent, A. A. Abbott, and C. Branciard, PRX Quantum 2, 030335 (2021).

^[17] C. Mukhopadhyay and A. K. Pati, Journal of Physics

- Communications 4, 105003 (2020).
- [18] C. Cardoso-Isidoro and F. Delgado, Symmetry 12, 10.3390/sym12111904 (2020).
- [19] C. Cardoso-Isidoro and F. Delgado, Journal of Physics: Conference Series 1540, 012024 (2020).
- [20] D. Deutsch, A. Ekert, R. Jozsa, C. Macchiavello, S. Popescu, and A. Sanpera, Phys. Rev. Lett. 77, 2818 (1996).
- [21] W. Dür and H. J. Briegel, Reports on Progress in Physics 70, 1381 (2007).
- [22] M. Araújo, C. Branciard, F. Costa, A. Feix, C. Giarmatzi, and Č. Brukner, New Journal of Physics 17, 102001 (2015).
- [23] G. Chiribella, M. Wilson, and H. F. Chau, Phys. Rev. Lett. 127, 190502 (2021).
- [24] D. Sych and G. Leuchs, New Journal of Physics 11, 013006 (2009).
- [25] P. Kómár, E. M. Kessler, M. Bishof, L. Jiang, A. S. Sørensen, J. Ye, and M. D. Lukin, Nature Physics 10, 582 (2014).
- [26] W. Zhang, T. van Leent, K. Redeker, R. Garthoff, R. Schwonnek, F. Fertig, S. Eppelt, W. Rosenfeld, V. Scarani, C. C.-W. Lim, and H. Weinfurter, Nature 607, 687 (2022).
- [27] S. Bratzik, S. Abruzzo, H. Kampermann, and D. Bruß, Phys. Rev. A 87, 062335 (2013).
- [28] D. Gottesman, T. Jennewein, and S. Croke, Phys. Rev. Lett. 109, 070503 (2012).

- [29] A. S. Cacciapuoti, M. Caleffi, F. Tafuri, F. S. Cataliotti, S. Gherardini, and G. Bianchi, IEEE Network 34, 137 (2020).
- [30] C. H. Bennett, D. P. DiVincenzo, J. A. Smolin, and W. K. Wootters, Phys. Rev. A 54, 3824 (1996).
- [31] W. Dür, H.-J. Briegel, J. I. Cirac, and P. Zoller, Phys. Rev. A 59, 169 (1999).
- [32] B. Olson, I. Hashmi, K. Molloy, and A. Shehu, Advances in Artificial Intelligence 2012, 674832 (2012).
- [33] C. H. Bennett, G. Brassard, S. Popescu, B. Schumacher, J. A. Smolin, and W. K. Wootters, Phys. Rev. Lett. 76, 722 (1996).
- [34] A. Miyake and H. J. Briegel, Phys. Rev. Lett. 95, 220501 (2005).
- [35] C. H. Bennett, D. P. DiVincenzo, J. A. Smolin, and W. K. Wootters, Phys. Rev. A 54, 3824 (1996).
- [36] S. Bravyi and A. Kitaev, Phys. Rev. A 71, 022316 (2005).
- [37] M. E. Beverland, A. Kubica, and K. M. Svore, PRX Quantum 2, 020341 (2021).
- [38] D. J. Weigand and B. M. Terhal, Phys. Rev. A 97, 022341 (2018).
- [39] C. H. Bennett, G. Brassard, C. Crepeau, R. Jozsa, A. Peres, and W. K. Wootters, Phys Rev Lett 70, 1895 (1993).
- [40] G. Bowen and S. Bose, Phys. Rev. Lett. 87, 267901 (2001).